MS109

Micromedia Limited

The contents of this microfiche are copyright by the publisher of the original document. Please contact the original publisher for guidance in copyright matters.

PM-1 3½"x4" PHOTOGRAPHIC MICROCOPY TARGET
NBS 1010a ANSI/ISO #2 EQUIVALENT

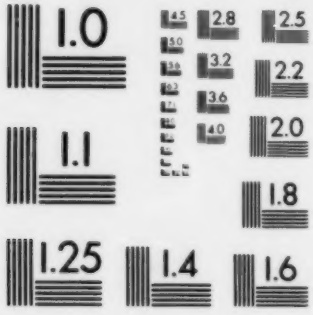

MICROCOPY RESOLUTION TEST CHART
NATIONAL BUREAU OF STANDARDS
STANDARD REFERENCE MATERIAL 1010a
(ANSI and ISO TEST CHART No. 2)

This statement was filmed with this document.
If the pages of the document are less clear than this statement it is due to the poor photographic quality of the document.

NATIONAL MICROGRAPHICS ASSOCIATION

24x

Energy, Mines and Resources Canada

Énergie, Mines et Ressources Canada

CANMET

Canada Centre for Mineral and Energy Technology

Centre canadien de la technologie des minéraux et de l'énergie

Metals Technology Laboratories

Laboratoires de la technologie des métaux

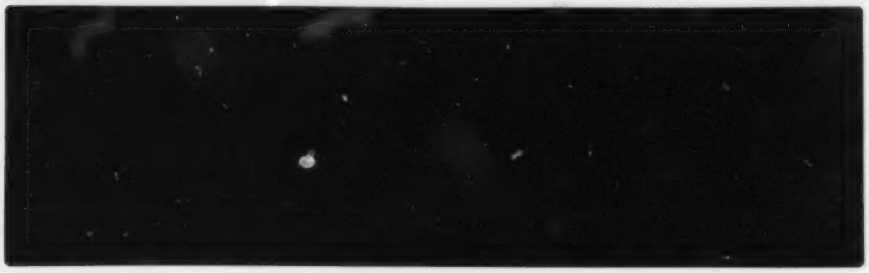

Canada

WELD CRACKING OF MONEL

M. SAHOO, V.E. MOORE, R.J. DAWSON* AND J.L. DION

MTL 89-41(TR)

16 pp

MICROMEDIA

CANMET

METALS TECHNOLOGY LABORATORIES
REPORT: MTL 89-41(TR)

WELD CRACKING OF MONEL

by

M. Sahoo, V.E. Moore, R.J. Dawson* and J.L. Dion

SUMMARY

Examination of weld cracks in a monel impeller casting showed that cracking was caused by bismuth.

---

* Technical Manager, Deloro Stellite Inc., Belleville, Ont.

89-05076/

LABORATOIRES DE LA TECHNOLOGIE DES MÉTAUX
RAPPORT: MTL 89-41(TR)

FISSURATION DES SOUDURES DANS L'ALLIAGE Ni-Cu (Monel)

par

M. Sahoo, V.E. Moore, R.J. Dawson* et J.L. Dion

RÉSUMÉ

L'examen des fissures dans les soudures d'une roue motrice coulée en alliage Ni-Cu (Monel), démontres qu'elles sont causées par la présence du bismuth.

INTRODUCTION

As part of the cost-shared project on high-strength monels, Deloro Stellite Inc. wanted to carry out the weld repair of a particular casting. To this end, a pump housing and an impeller were cast at MTL's experimental foundry. Moulds for these two castings were prepared at Deloro using pepset sand.

Melting was carried out in the tilt-type 250 kg induction furnace lined with alumina. A wash heat had been done prior to melting monel.

The impeller casting (Fig. 1) was weld repaired at Deloro using monel 60 electrodes. The welding parameters are given in Table 1. Unfortunately, each weld-repaired area showed cracks even when observed using a magnifying glass. It may be noted that the weldability of monels cast previously at MTL had been evaluated using the weldability test specified in ASMT B369-88 for cupro-nickels and was found to be satisfactory.

The weld repaired impeller was sent to MTL to investigate the cause for cracking.

BACKGROUND

The normal practice in the preparation of monel was to use either virgin metals and master alloys or a mixture of in-house returns, virgin metals and master alloys. The latter method was used for melt #3122 to cast the impeller and pump housing. In-house returns from four different melts whose compositions were found to be satisfactory were used for melt #3122. One such return was melt #3046. The tensile properties of this melt had not been determined during the time of casting the impeller because of the delay in getting the tensile specimens machined. At a later date, the tensile properties were found to be unsatisfactory and the UTS and % elongation did not meet the requirements specified in ASTM A744/A744M-86. The UTS and % elongation were about 340 MPa and 9%, respectively By contrast, mechanical properties of all the previous melts exceeded the ASTM specifications (450 MPa UTS, 170 MPa YS and 25% elongation). It was, therefore, of interest to investigate the cause of low ductility of melt #3046 followed by investigation of the weld cracking of the impeller in melt #3122.

RESULTS AND DISCUSSION

Photographs of the impeller with all the weld repaired regions are shown in Fig. 2(a) and (b). A couple of weld beads from the impeller were sectioned for metallography. Figures 3 and 4 show the optical micrographs of the fusion zone and parent metal. Cracking appears to be intergranular in the parent metal. Cracks were observed in the fusion zone in Fig. 3 and 4.

From our previous experience with weldability of copper-base alloys, this type of weld cracking was thought to be caused by some impurity, probably of the low melting type such as lead. Chemical analysis of melts #3046 and 3122 showed the lead content to be low (Table 2). In order to detect the low levels of impurity elements, it was decided to examine the fracture surface of the tensile specimen from melt #3046 in the electron-microprobe analyser before examining the welds. As shown in Fig. 5-7, only bismuth was detected at grain boundaries and interdendritic areas. The presence of bismuth was also observed in the polished section of the tensile samples. Bismuth is known to have adverse effect on ductility and weldability of copper-base alloys.

Examination of polished sections of the weld bead in the electron microprobe did not reveal the presence of bismuth. Instead, strong peaks for Al, Si and Na were obtained from some faceted particles. X-ray maps showed these to be alumina, silicon carbide and probably sodium-aluminum-silicate (Fig. 8). It is possible that alumina and sodium have originated from the alumina refractory lining.

In another attempt, a weld bead was fractured and examined in the electron microprobe. Energy dispersive analysis showed strong peaks for bismuth (Fig. 9-10). The X-ray maps for bismuth show that the bismuth content of melt #3122 is less than that of melt #3046. This is to be expected because only 35 kg returns of #3046 were added to prepare a melt of 270 kg monel.

These results show that bismuth might have been the cause of weld cracking in monel. For further verification, a weldability test plate from melt #3046 was sent to Deloro Stellite to carry out weld repair employing the method used for the impeller. Each weld bead cracked.

Chemical analysis of melts #3046 and 3122 gave bismuth contents of 0.41% and 0.045%, respectively.

Average mechanical properties of three tensile specimens from melt #3122 were 477 MPa UTS, 194 MPa 0.2% yield strength and 25% elongation. These values are higher than these obtained from melt #3046 probably because of the reduced bismuth content. It may also be noted that despite such bismuth content, the ASTM specified mechanical properties have been met.

The reasons for this high bismuth content in melt #3046 are not yet clear. To-date, about 25 monel melts have been prepared in MTL's experimental foundry. This is the only melt which had this unusually high bismuth level. Pure bismuth is not kept in the usual storage area where virgin metals and master alloys are stored. Virgin metals and master alloys used to prepare melt #3046 have been used for other melts which did not exhibit this unusual behaviour.

Table 1. Weld repairing procedure for impeller casting in monel.

Process	Manual TIG
Material	Monel 60, 1.6 mm (0.062 in.) diam (INCO electrode)
Preheat temperature	Nil (room temperature)
Post weld heat treatment	600°F
Shielding gas and flow rate	Argon, 30 cfh
Current and polarity	Direct current
Amperage	100-125 A
Travel speed	3.4 mm/s (8 ipm)
Inspection	Liquid penetrant

Table 2. Chemical analysis (wt %) of monel

Melt No.	Ni	Cu	Fe	Mn	Si	Nb	C	Mg	Ti	Pb	S	P	Bi
3046*	64.1	29.9	1.3	0.9	1.56	1.50	0.19	0.024	0.1	0.004	0.0016	<0.002	0.41
3122**	66.2	28.2	1.49	0.81	1.49	1.60	0.18	0.016	0.1	<0.01***	<0.001	0.005	0.045

* Prepared from virgin metals and master alloys. Tensile specimen showed 8-10% elongation instead of >25% elongation.

** Impeller casting. Returns from #3046 (35Kg) were used to prepare a melt of 270Kg.

*** Deloro analysis.

Fig. 1. Photograph of pump impeller showing the gating and risering system. (neg 18948-4)

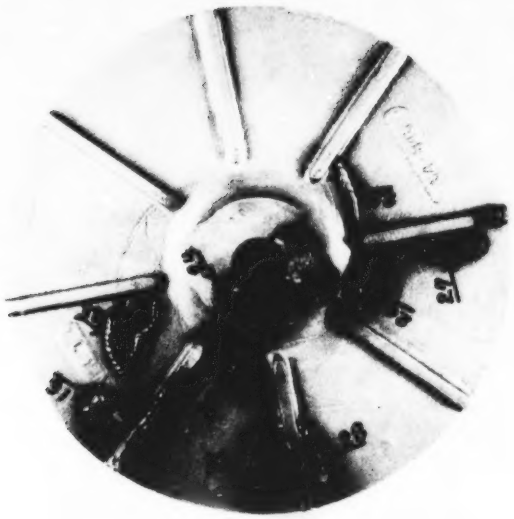

[(a) neg 19111]

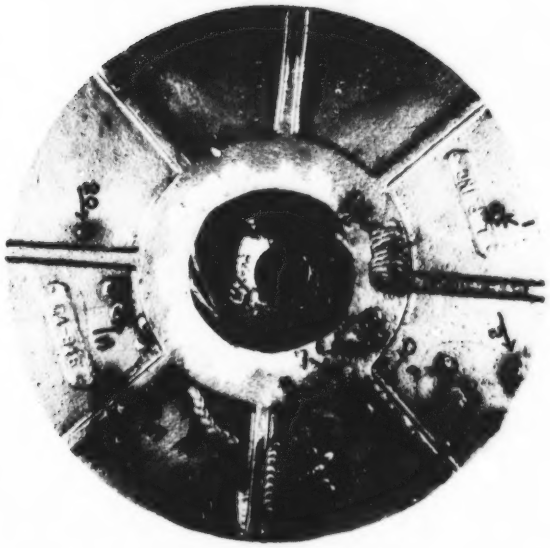

[(b) neg 19112]

Fig. 2. Weld repair done at random on both sides of the impeller.

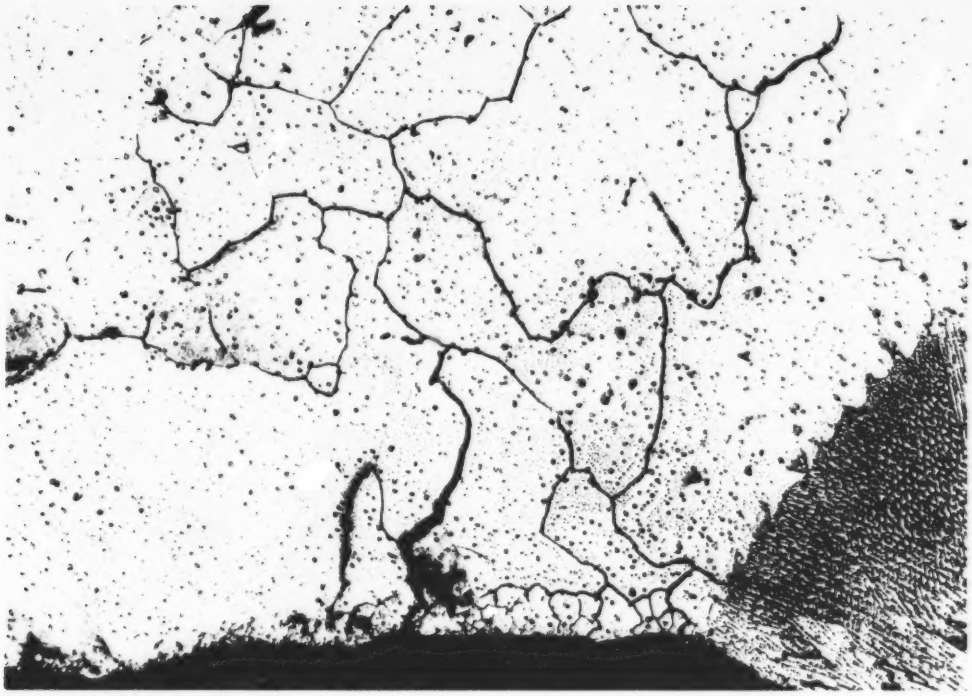

[(a) neg 19315]

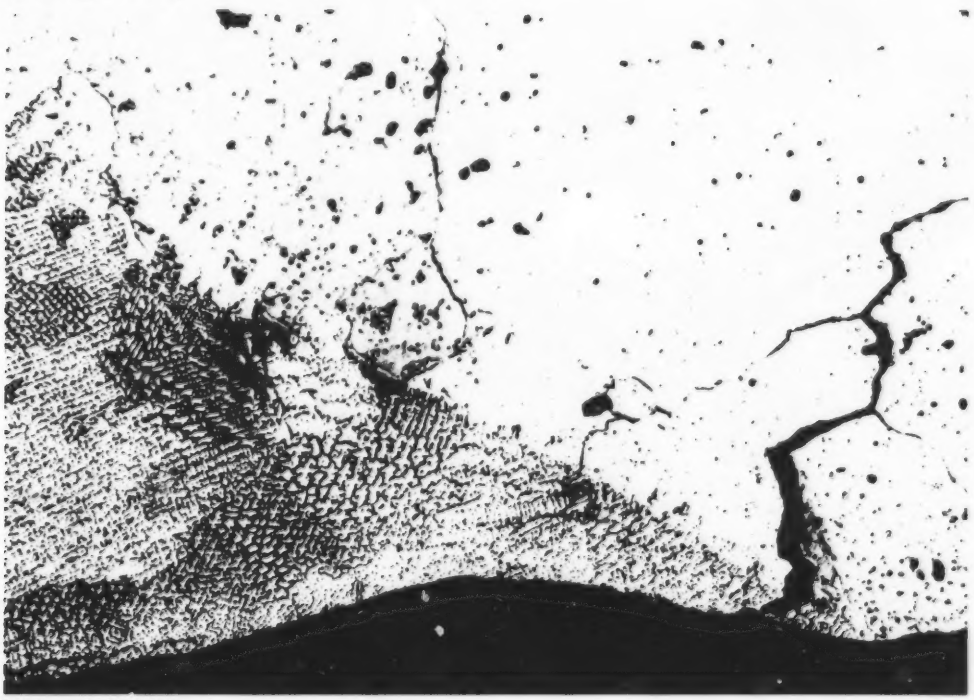

[(b) neg 19316]

Fig. 3. Optical micrographs showing cracks near weld repair #13.

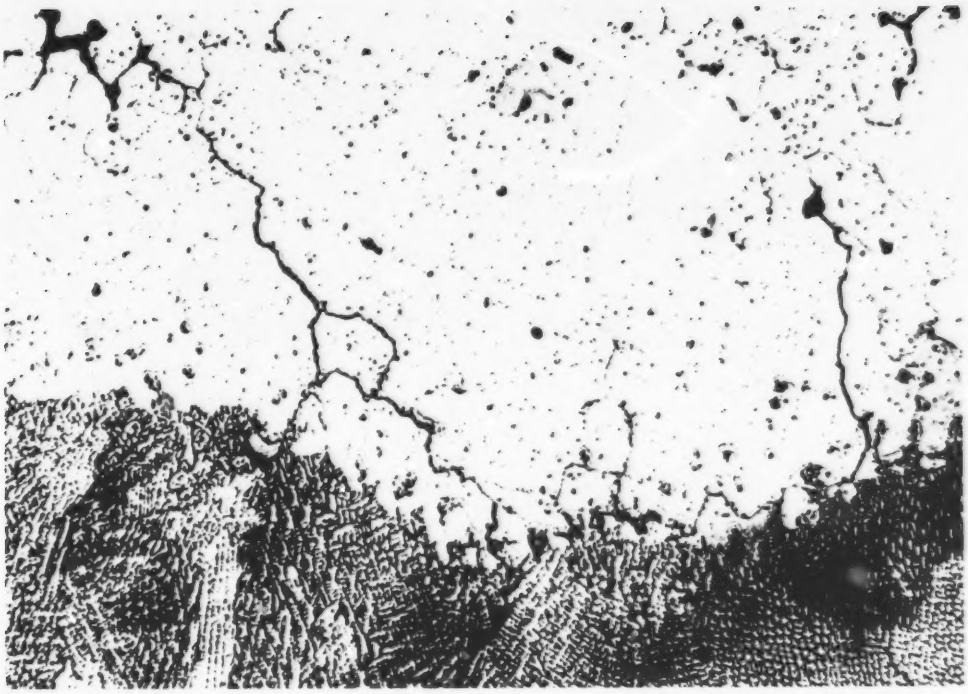

[(c) neg 19317]

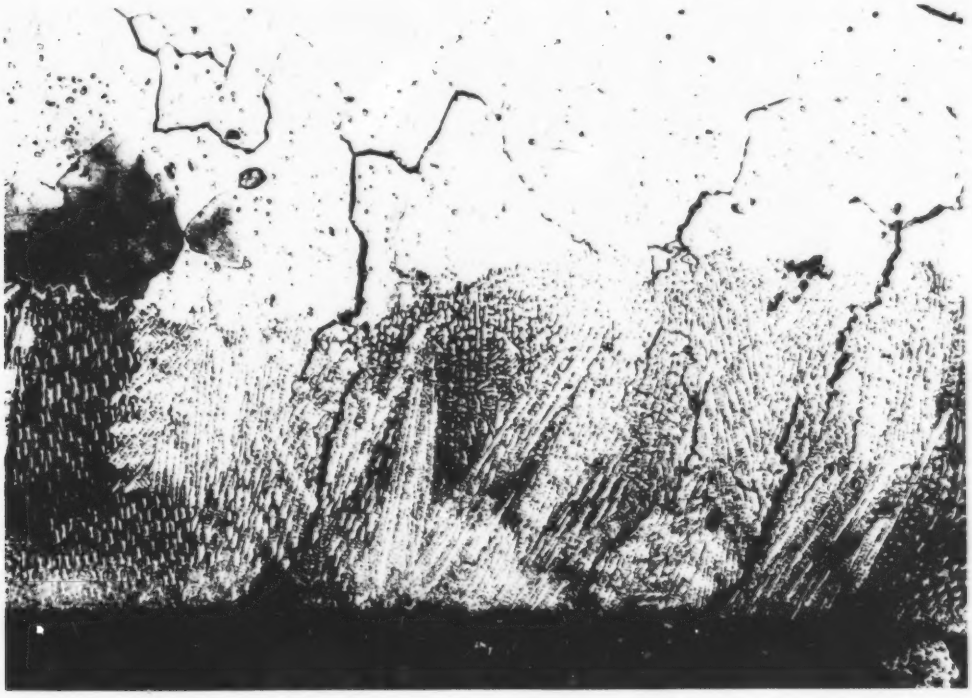

Fig. 4. Optical micrograph of weld repair #21 showing cracks in the fusion zone and parent metal. (neg 19318)

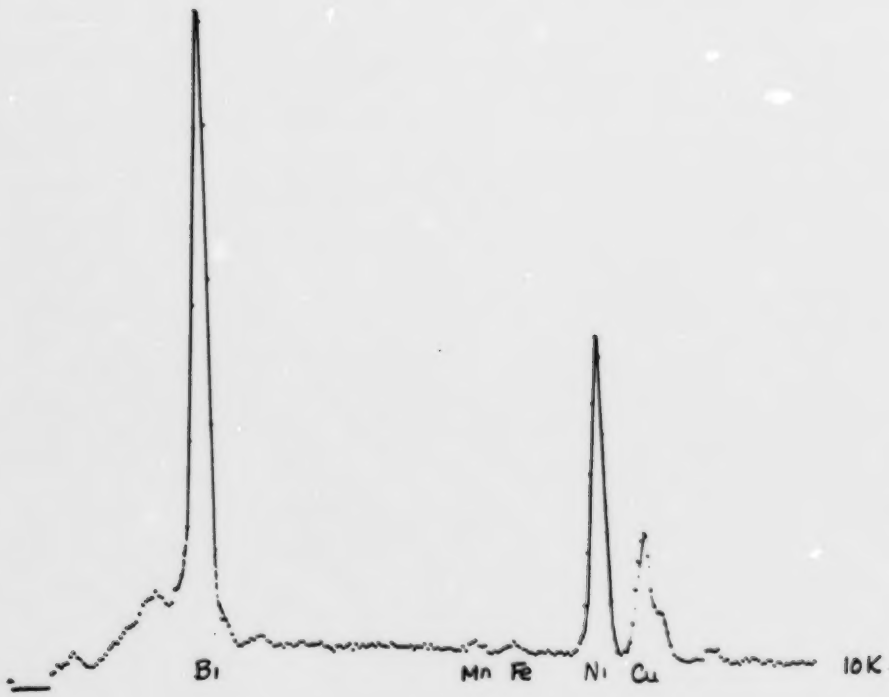

Fig. 5. X-ray intensity of elements in melt #3046. (neg 19250)

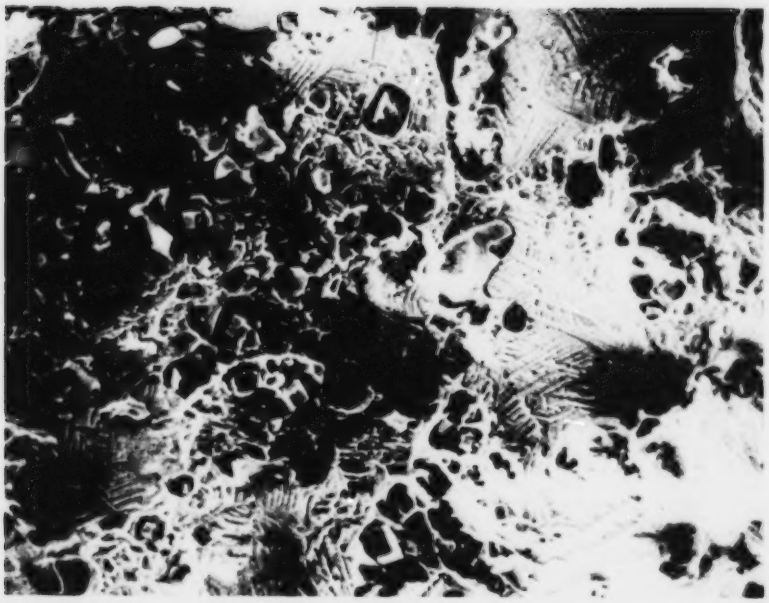

(a) fracture face, x 400. (neg 19251)

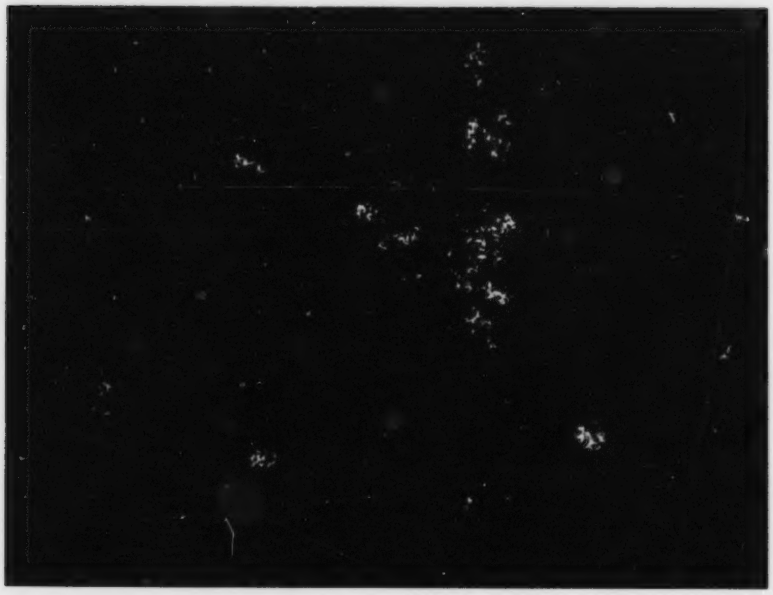

(b) X-ray map for bismuth. (neg 19252)

Fig. 6. Fracture face of melt #3046 tensile specimen as seen in the electron-microprobe analyser.

(a) fracture face, x1600. (neg 19255)

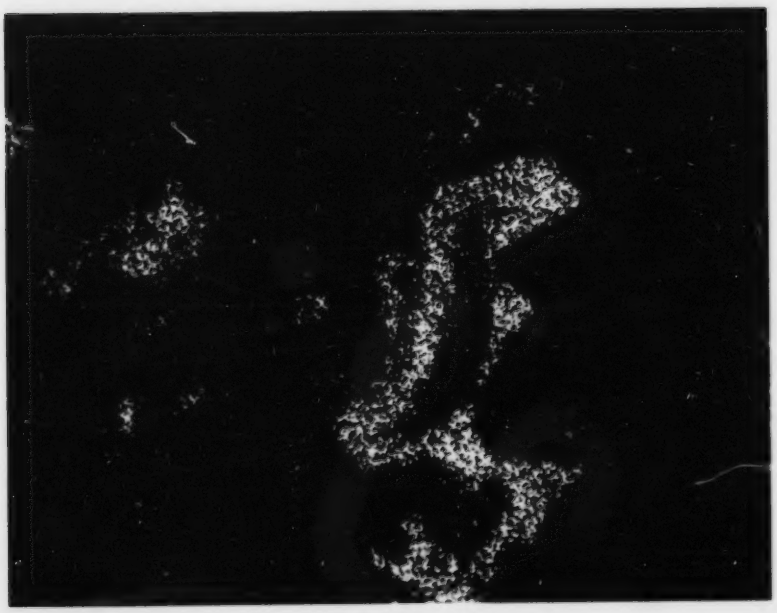

(b) X-ray map for bismuth. (neg 19256)

Fig. 7. Fracture face of melt #3046 tensile sample as seen in the electron-microprobe analyser.

Fig. 8. Secondary electron image of inclusions in a polished section of weld repaired monel as seen in the electron-microprobe analyser. (negs 19257 and 19258)

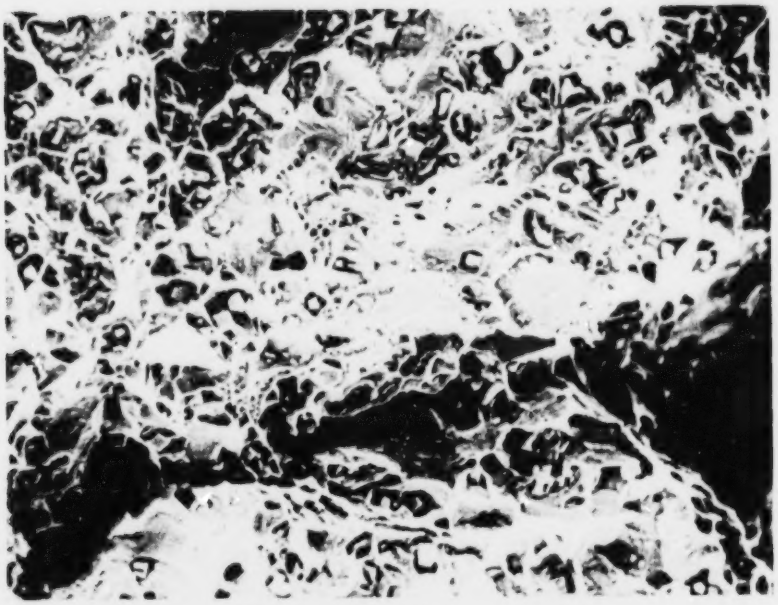

(a) fracture face, x 400. (neg 19259)

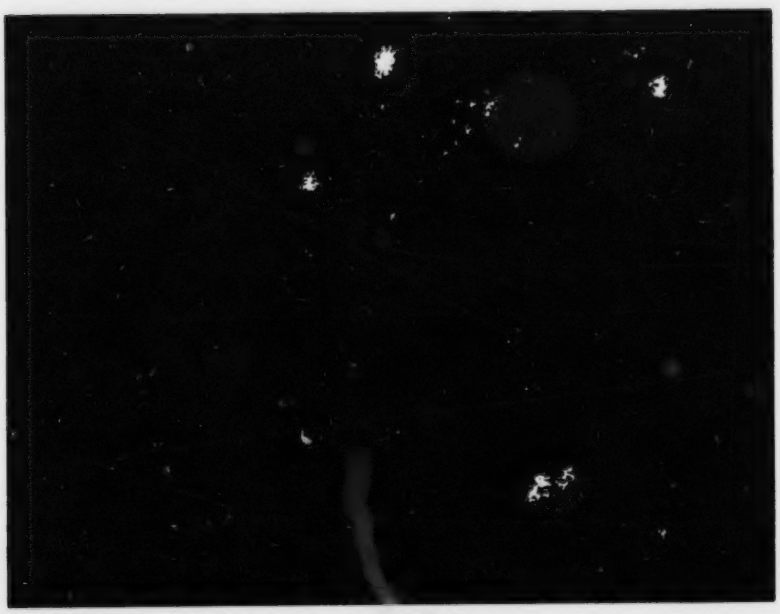

(b) X-ray map for bismuth. (neg 19260)

Fig. 9. Fracture face of the weld repaired monel as seen in the electron-microprobe analyser.

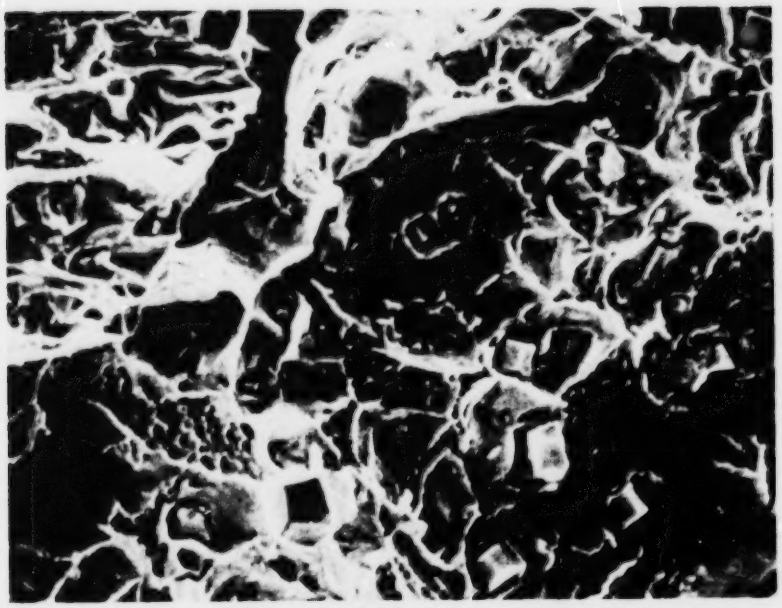

(a) fracture face, x 800. (neg 19261)

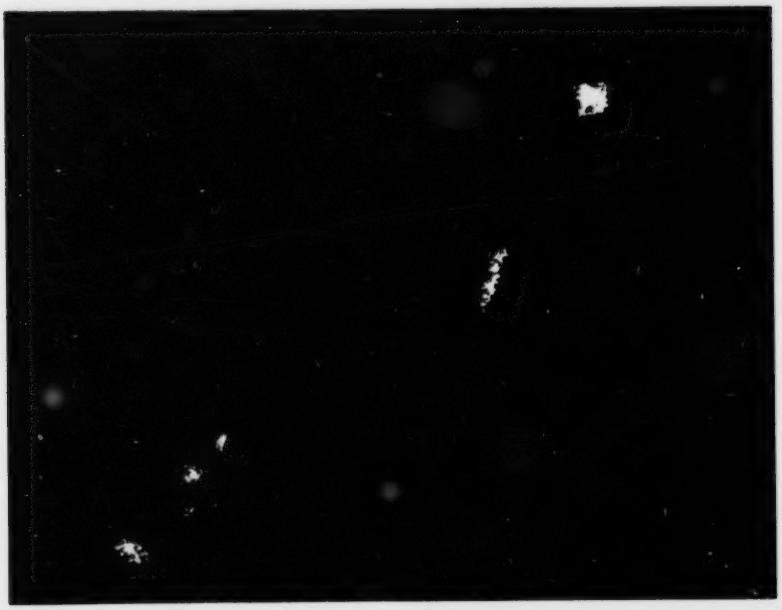

(b) X-ray map for bismuth. (neg 19262)

Fig. 10. Fracture face of weld repaired monel as seen in the electron-microprobe analyser.